Automated design of bone-preserving, insertable, and shape-matching patient-specific acetabular components

Garner, Eric; Meynen, Alexander; Schey, Lennart; Wu, Jun; Zadpoor, A.A.

Citation (APA)
Garner, E., Meynen, A., Schey, L., Wu, J., & Zadpoor, A. A. (2024). Automated design of bone-preserving, insertable, and shape-matching patient-specific acetabular components. *Journal of Orthopaedic Research*. https://doi.org/10.1002/jor.25927

Important note
To cite this publication, please use the final published version (if applicable).
Please check the document version above.

RESEARCH ARTICLE

Automated design of bone-preserving, insertable, and shape-matching patient-specific acetabular components

Eric Garner[1] [ORCID] | Alexander Meynen[2] | Lennart Schey[2] | Jun Wu[3] |
Amir A. Zadpoor[1]

[1]Department of Biomechanical Engineering, Delft University of Technology, Delft, The Netherlands

[2]Department of Development and Regeneration, Faculty of Medicine, Institute for Orthopedic Research and Training (IORT), KU Leuven, Leuven, Belgium

[3]Department of Sustainable Design Engineering, Delft University of Technology, Delft, The Netherlands

Correspondence
Eric Garner, Department of Biomechanical Engineering, Delft University of Technology, Delft, 2628 CD, The Netherlands.
Email: ericgarner92@gmail.com

Abstract

Effective treatment of large acetabular defects remains among the most challenging aspects of revision total hip arthroplasty (THA), due to the deficiency of healthy bone stock and degradation of the support columns. Generic uncemented components, which are favored in primary THA, are often unsuitable in revision cases, where the bone-implant contact may be insufficient for fixation, without significant reaming of the limited residual bone. This study presents a computational design strategy for automatically generating patient-specific implants that simultaneously maximize the bone-implant contact area, and minimize bone reaming while ensuring insertability. These components can be manufactured using the same additive manufacturing methods as porous components and may reduce cost and operating-time, compared to existing patient-specific systems. This study compares the performance of implants generated via the proposed method to optimally fitted hemispherical implants, in terms of the achievable bone-implant contact surface, and the volume of reamed bone. Computer-simulated results based on the reconstruction of a set of 15 severe pelvic defects (Paprosky 2A-3B) suggest that the patient-specific components increase bone-implant contact by 63% (median: 63%; SD: 44%; 95% CI: 52.3%–74.0%; RMSD: 42%), and reduce the volume of reamed bone stock by 97% (median: 98%; SD: 4%; 95% CI: 95.9%–97.4%; RMSD: 3.7%).

KEYWORDS
acetabular component, automated design, insertability, patient-specific, revision total hip arthroplasty

1 | INTRODUCTION

Total hip arthroplasty (THA) is among the most commonly performed surgical procedures, with 182 surgeries performed per 100 000 population in 2019, according to OECD reports, rising 22% since 2009.[1] This increase is expected to foreshadow a substantial rise in revision THA in the coming decades.[2] Revision procedures present significant challenges due to the loss of healthy bone stock and degradation of the load-bearing structures.[3] Acetabular reconstruction, in particular, requires careful preoperative planning and may involve

a variety of approaches, depending on the nature and severity of the defect.[4]

In many revision cases, standard hemispherical components (with or without joint centroid offset) may not provide adequate bone-implant contact for biological fixation, without significant reaming of the remaining bone stock.[5] In these cases, surgeons have generally been limited to cemented options.[4] More recently, specialized products, such as the trabecular metal reconstruction system (TMARS) offer improved implant stability by introducing metal augments in bone-deficient areas and cementing them to the acetabular cup intra-operatively.[6]

Augments effectively extend the surface of the component to better match the defect morphology. They are, in a sense, built-in-place patient-specific implants. The use of porous metal augments has revolutionized the treatment of severe acetabular defects over the last two decades, with midterm reports showing excellent survivability.[7,8] Nonetheless, their use remains labor-intensive and is limited in its ability to accurately match the defect geometry, due to the finite set of augment shapes and sizes available, and the nature of the surgical procedure.[9]

Patient-specific acetabular components, on the other hand, are designed to precisely match bone morphology. This approach offers the potential for preoperative in silico structural analysis, as well as improved implant stability and reduced bone reaming. However, the typical approach is resource-intensive and involves manual design and analysis by expert engineers, surgeons, and technicians, thus limiting its widespread adoption. Moreover, existing patient-specific systems, such as the custom triflange acetabular component (CTAC), fixate the implant at multiple sites on the outer surface of the pelvis, requiring a larger operating window and creating additional challenges in terms of positioning and stabilization.[10] This compromise is generally preferred when alternative generic or patient-specific systems would result in insufficient remaining bone stock to support the transmitted loads.

Recently, we have proposed an algorithm that can automatically generate shape-matching components while guaranteeing their insertability.[11] When applied to the design of patient-specific acetabular cups, this approach enables an automated design workflow based on CT scan defect reconstructions, that can maximize bone-implant interface contact while minimizing the volume of bone to be reamed.

The aim of this study, therefore, is to apply the above-mentioned algorithm to automatically generate implants for a representative sample of pelvic defects and to quantify the potential performance improvement with respect to traditional hemispherical components, in terms of bone-implant contact surface and reaming volume.

The remainder of this paper is organized as follows: Section 2 reviews the design algorithm and relevant performance metrics. Section 3 presents numerical results and analysis. Finally, Section 4 concludes with a discussion on the limitations of the proposed method and a qualitative comparison to other patient-specific systems.

2 | METHODS

2.1 | Data set of acetabular defects

A specific sample of 15 acetabular defects was selected from a data set of 90 3D models reconstructed from patient data by Meynen et al.[12] The study, which was approved by the ethical committee of the university hospital Leuven (S61746), used unilateral CT scans of revision THA patients, after excision, and before reimplantation. The sample set used in this study was selected from the data set based on the results of a statistical shape model analysis,[13] accounting for 73% of the total shape variance. For each of the first five shape modes identified, three real defects were selected from the data set; one for each of the mean and mean ± one standard deviation.

2.2 | Automated design of patient-specific cups

Patient-specific acetabular components were computationally generated using an algorithm presented in Garner et al.[11] The design strategy aims to optimize the outer geometry of the component to best match the morphology of the acetabular defect, while ensuring that the optimized structure is insertable through rigid body motion, that is, without damaging the surrounding bony tissue.

#### 2.2.1 | Interface matching and insertability

An implant with surface geometry perfectly complementary to the acetabulum would produce ideal bone-implant contact. However, such an implant would not necessarily be insertable. The design strategy proposed in Garner et al.[11] addresses this issue by identifying the areas that inhibit insertion along a certain path, as shown in Figure 1.

Specifically, the algorithm simulates the implant in its inserted configuration, and assesses the surface translations induced by a small extractive movement along a specific path. Generally speaking, if the translation is *into* the interface at any point, then local interference is detected, and the implant is deemed uninsertable along this insertion/extraction path.

Constrained by this insertability requirement, the algorithm iteratively modifies the implant geometry and the insertion path to find an insertable design, while minimizing changes to the implant's shape. Mathematically, we formulate an optimization problem in which the interface geometry, described by ρ, is modified to minimize a shape change function F_S, while respecting an insertability constraint:

$$\underset{\rho(\boldsymbol{p},\boldsymbol{\theta})}{\text{minimize}}\, F_s = \frac{1}{n}\sum_{i=1}^{n}|d(\boldsymbol{b}_i, S_0)| \quad s.t. \quad r_b^n(\boldsymbol{p},\boldsymbol{\theta}) > r_{\min}^n(\boldsymbol{p},\boldsymbol{\theta}),$$

where $d(\boldsymbol{b}_i, S_0)$ is the closest distance from a point $\boldsymbol{b}_i$ on the evolving body surface to a point cloud describing the original geometry S_0. $(\boldsymbol{p}, \boldsymbol{\theta})$ describes the insertion direction in terms of translation and
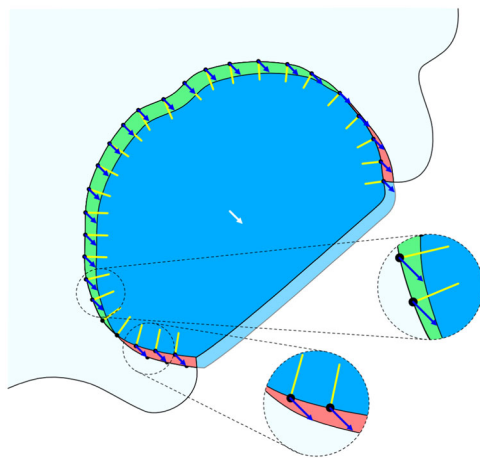
FIGURE 1 A body-cavity system before and after a small body movement in the direction shown by the arrow. Clearance and interference are displayed in green and red, respectively. Local cavity surface normals are shown in yellow. Sample body surface vertices in areas with interference are displaced in the negative normal direction, while body surface vertices in areas with clearance are displaced in the positive normal direction.

FIGURE 2 An automatically generated acetabular component corresponding to the acetabular defect shown in Figure 3. The acetabulum-side surface is optimized to fit the defect geometry, while the outer geometry is designed to ensure accurate positioning of the synthetic joint.

rotation vectors p and θ, and $r_{\min}^n$ is a minimum local normal displacement defined by the local tangential displacement r_t^t and curvature κ_b:
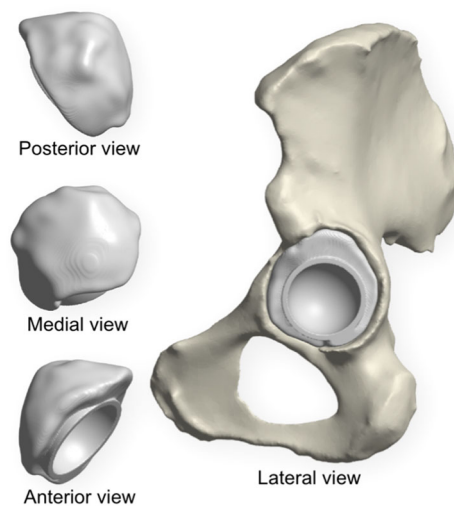
$$r_{\min}^n = \begin{cases} \kappa^{-1} - \sqrt{\dfrac{\kappa^{-2}\left(r_b^t(p,\theta)\right)^2}{\kappa^{-2} - \left(r_b^t(p,\theta)\right)^2}}, & \kappa > 0, \\ \\ 0, & \text{otherwise.} \end{cases}$$

We refer to Broekhuis et al.[10] for a detailed explanation of the optimization problem and solution strategy.
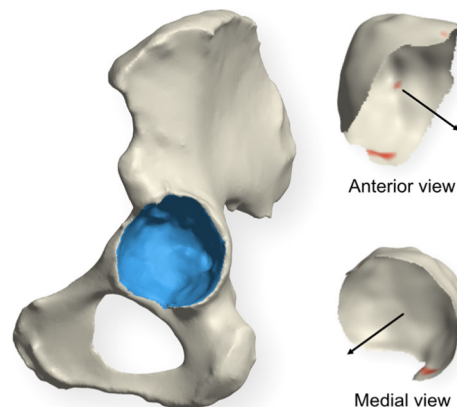
2.2.2 | Anatomical restoration

The anatomical features surrounding the acetabulum, such as the acetabular margin and supraacetabular groove, are obtained from a statistical shape model reconstruction of the healthy pelvis.[13] This is achieved by superimposing the defect and reconstruction geometry and extracting the volumetric difference. The reconstructed healthy pelvis also provides the optimal center of rotation for the artificial joint. Note that this could equally be achieved from contra-lateral imaging, if available.

The reconstructed acetabular surface is then replaced by a hemisphere component, so as to provide support for a standard 36 mm polyethylene or ceramic liner (Figure 2). At this stage, additional features, such as friction or bone ingrowth-enhancing features, and liner-retaining lips or grooves may be added. Holes for locking screws can be included as needed, and strategically placed to target healthy bone, based on CT data. Note that the increased surface contact and the irregular interface geometry likely decrease


FIGURE 3 Left: A sample pelvis with acetabular surface highlighted. Right: The extracted acetabulum with insertion-inhibiting areas highlighted for the insertion direction shown.

the load bearing on fasteners, though this aspect is beyond the scope of this work.

2.3 | Reference cup selection

In this study, standard hemispherical components were used as a performance benchmark. While hemispherical components may not always represent the best option in revision cases, alternative approaches using generic components introduce too many additional variables for a direct performance comparison.

To ensure optimal sizing and placement of the spherical component, an automated selection and implantation strategy was designed. First, the centroid of the defect was identified as the
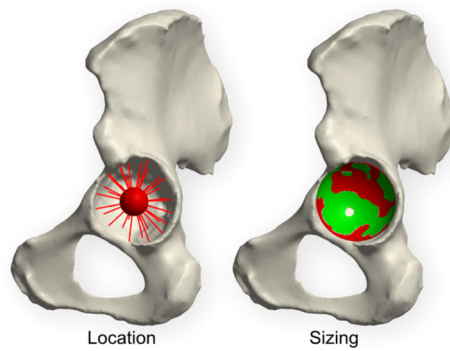
FIGURE 4 Selection of the reference hemispherical cup. The joint centroid is located by projecting rays onto the acetabulum (red lines). The cup radius is obtained as the minimum radius which results in a contact surface of 50% with respect to the area of the hemisphere. The contact and noncontact surfaces are shown in green and red, respectively. The white region along the central segment is a discontinuity created by the associated reaming process.

FIGURE 5 Bone–implant interface contact for the reference hemispherical component (left) and patient-specific optimized component (right). Contact regions and no-ingrowth regions are shown in green and red, respectively. Regions with interface gap smaller than 50 μm are shown in yellow.

spatial coordinates that minimize the radial distance variance of rays projected onto the acetabulum, as shown in Figure 4 (left). The component radius was then chosen to provide a contact of 50%, with respect to the surface area of the component (Figure 4, right). In many cases, achieving the desired contact ratio created or enlarged an already existing central segment discontinuity. In cases of extreme bone deficiency, 50% contact was not always possible. In these cases, the maximum achievable contact ratio was used instead.
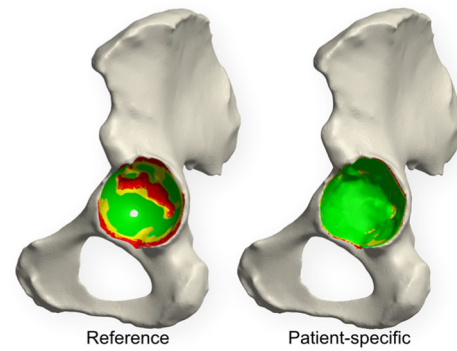
2.4 | Performance analysis

Performance was quantified based on two metrics: bone-implant interface contact and volumetric bone loss. Infection or inflammation-related failure, and instability-related issues are the most common diagnoses associated with implant failure.[14–16] While neither can be directly accounted for at the time of implantation, both are thought to be related to initial interface contact and/or volumetric bone loss.[8,17,18]

2.4.1 | Bone-implant interface contact

Interface contact was quantified in terms of the contact surface area (within 50 μm) and the fractional contact area relative to the surface area of the acetabulum before resection. The total area with gap larger than 1 mm, for which no bone ingrowth is expected,[19] was also measured. Figure 5 shows the contact and no-ingrowth regions for the patient-specific and reference hemispherical implants, corresponding to the defect in Figure 4. The relative improvement in terms of interface contact A^{rel} is defined as

$$A^{rel} = \frac{A_c^{p.s.}}{A_c^{ref}} - 1,$$

where A_c^{ref} and $A_c^{p.s.}$ are the bone-implant contact area for the reference hemispherical and patient-specific designs. In Figure 5, the minor interface gaps correspond to small pitting along the acetabular surface, which are too small for the design algorithm or additive manufacturing process to capture. The only exception is the larger cavity on the posterior–inferior surface, which could not be filled without sacrificing insertability, as highlighted in Figure 3.

2.4.2 | Volumetric bone loss

The total bone loss resulting from the required reaming was evaluated by simulating the resection process and measuring the total change in bone volume through high-resolution voxelization (1 million voxels). Figure 6 shows the resection depth together with original and reamed pelvis geometry, corresponding to the defect shown in Figure 3.

The relative reduction in bone loss V_{loss}^{rel} is defined as

$$V_{loss}^{rel} = \frac{\left(V_{loss}^{ref} - V_{loss}^{p.s.}\right)}{V_{loss}^{ref}} - 1,$$

where V_{loss}^{ref} and $V_{loss}^{p.s.}$ are the volume of bone resected for the reference and patient-specific components, respectively.

2.4.3 | Statistical analysis

In this study, the objective was to determine if the proposed patient-specific implants offer a meaningful performance improvement compared to generic hemispherical components. To that end, the bone-implant interface contact ratio and volumetric bone loss metrics were measured for each of the reference and patient-specific designs. Results were collated as matched pairs for each of the 15 sample defects. Statistical significance was reported for paired
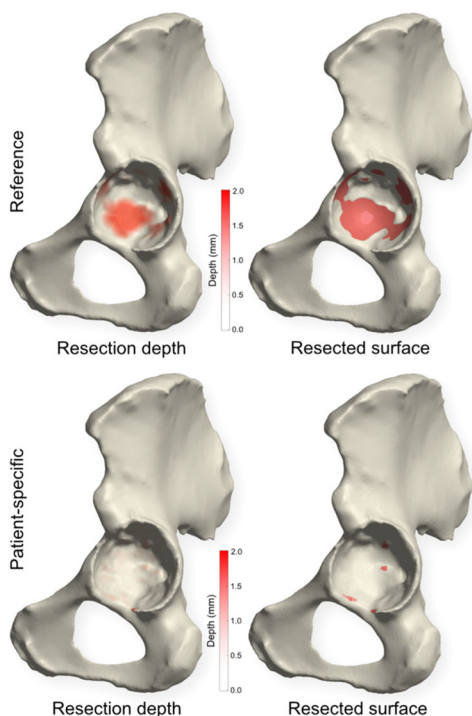
FIGURE 6 Resection depth (left) and the resected surface (right) for the reference hemispherical (top) and patient-specific optimized (bottom) components, for the defect shown in Figure 3.

sampled t tests with one-tailed H_1 hypothesis. To assess the strength of the performance improvement, Cohen's d effect size was also reported. In addition, performance improvements were compared based on the Paprosky defect classification of the sampled defects.

3 | RESULTS

Analysis of the 15 defect cases sampled suggest significant improvement in terms of both metrics. With respect to interface contact, a mean improvement of 63% was observed, compared to the reference hemispherical implants (median: 63%; SD: 44%; 95% CI: 52.3%–74.0%; RMSD: 42%). In terms of bone loss, a mean reduction of 97% was observed (median: 98%; SD: 4%; 95% CI: 95.9%–97.4%; RMSD: 3.7%).

Paired sample t tests with one-tailed H_1 hypothesis suggest strong statistical significance, with $p = 0.00002$, and $p = 0.001$, respectively. In addition, the effect sizes were $d = 2.04$ and $d = 0.92$. This suggests that meaningful improvement in terms of both metrics can be expected when using the proposed design strategy compared to hemispherical cups for similar defect types (2A-C, 3A-B). Results for each defect sampled are presented in Figures 7–8 and Table 1.

3.1 | Impact of defect type

To assess the impact of the defect type on the results, the sample defects were divided into type 2 and type 3 subgroups, and p-values

were computed for a t test with two-tailed H_1. The resulting p values were 0.14 and 0.82, with respect to the contact area and bone loss metrics, respectively. This suggests no statistical significance in support of the hypothesis that the defect type has an impact on the mean performance improvement of the proposed method, compared to the benchmark hemispherical cups. Nonetheless, the structural impact of the bone loss due to reaming may be more significant for type 3 defects, as the load bearing capacity is almost certainly lower, both pre- and postoperatively. It should also be noted that subtypes (A/B/C) may affect the performance too, though not enough data is available for analysis.

4 | DISCUSSION

The primary aim of this study was to apply the proposed computational algorithm to the design of patient-specific acetabular cups for use in THA and to compare their performance to standard hemispherical components in silico. A statistical analysis based on the proposed interface contact and bone loss performance metrics suggests that the patient-specific designs perform significantly better than their generic counterparts. This fairly predictable result makes a strong case for the use of patient-specific components as an alternative to generic components.

Beyond the performance metrics evaluated in this study, patient-specific implants offer several additional advantages. Studies suggest that patient-specific implants can contribute to lowering overall costs, surgical time, and patient recovery time.[20–22] In terms of material and overhead costs, patient-specific implants eliminate the need for maintaining a large inventory of acetabular components in various sizes and shapes.[21] Nevertheless, this comes at the expense of additional pressure on manufacturers in terms of data collection, design resources, production capacity, lead time, and logistics.

Another potential clinical advantage is operating time reduction. Patient-specific cups are designed based on the patient's specific anatomy, which allows for a more precise and efficient surgical procedure. Studies investigating the impact of patient-specific implants and tooling for knee arthroplasty show a clear reduction in operative time owing to the elimination of iterative intraoperative adjustments.[20,21] This observation likely also applies to acetabular components, where the labor-intensive task of fitting and cementing porous metal augments also contributes to operative time.

In addition to these benefits, the irregular geometry of patient-specific implants, such as the ones shown in this study naturally stabilizes the component in the target position through a poke-yoke effect. This reduces reliance on adjunct screws, and ensures accurate positioning of the component, as well as the joint's center of rotation.

Many of the aforementioned advantages are not unique to the proposed patient-specific implant design strategy. A qualitative comparison with commercially available solutions is, therefore, warranted. In recent years, several product lines have been introduced to address the shortcomings of generic acetabular cups, each with its own benefits and drawbacks. Existing products largely
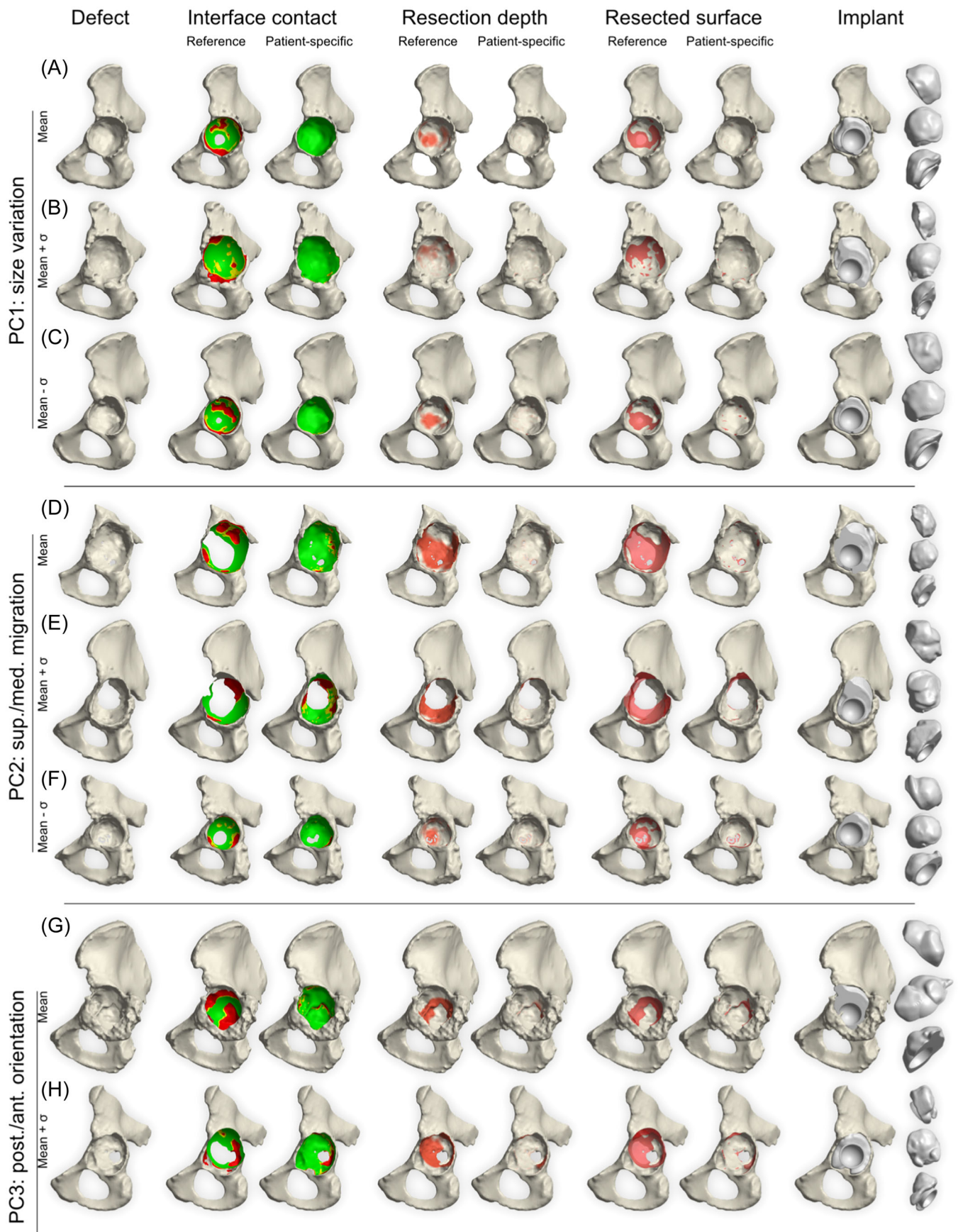
FIGURE 7 Results of the performance analysis for defects 1–8, shown in the left column. For each metric, the reference and patient-specific component performance are shown side-by-side.
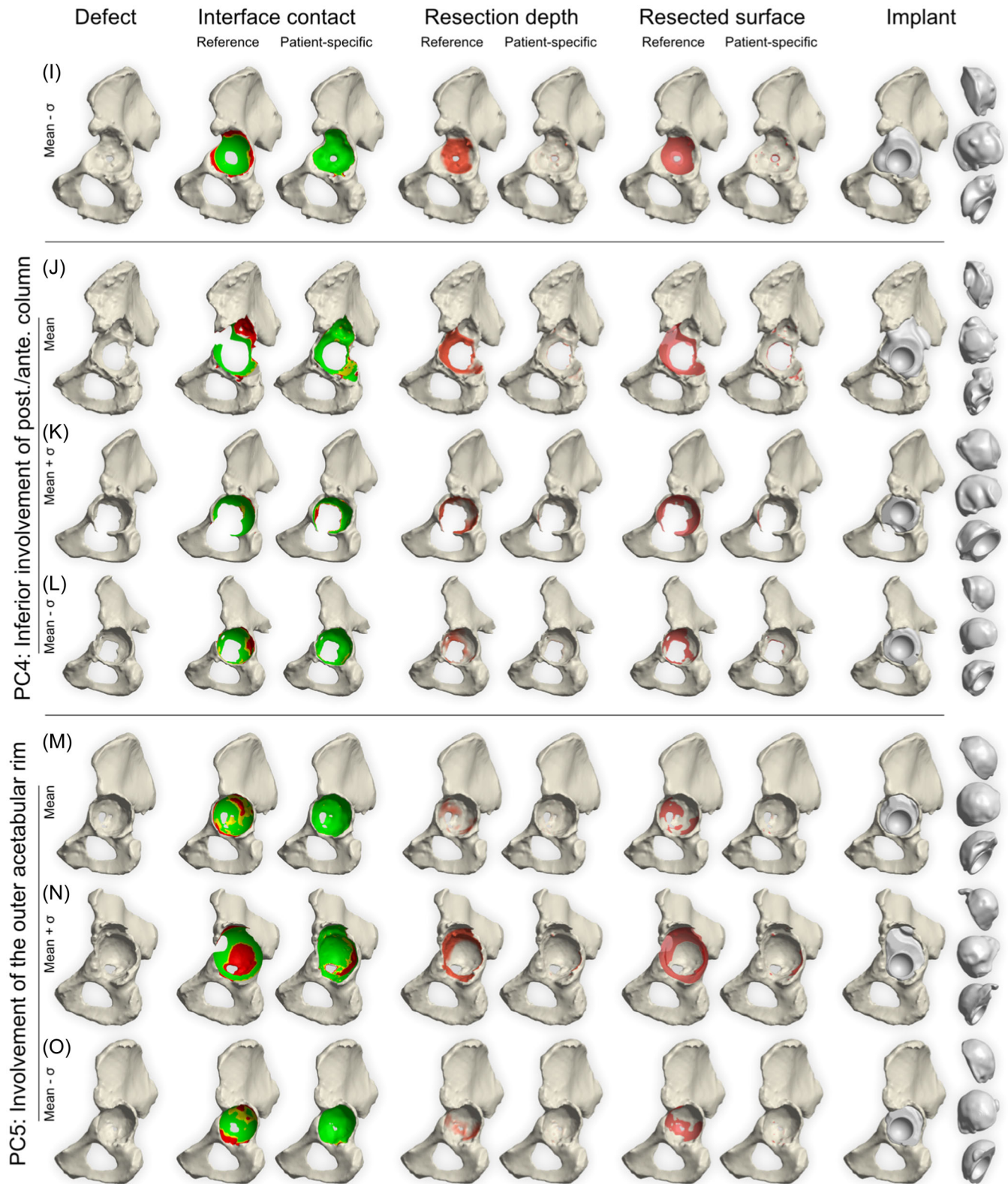
FIGURE 8 Results of the performance analysis for defects 9 through 15, shown in the left column. For each metric, the reference and patient-specific component performance are shown side-by-side.

TABLE 1 Results of the performance analysis for all the defects sampled.

Figure	Morphological variation	Stat. shape mode	Paprosky class.	Reference component		Patient-specific component		Difference	
				Contact ratio	Bone loss (mm³)	Contact ratio	Bone loss (mm³)	Contact ratio	Bone loss (mm³)
7(a)	Defect size	1	2B	42%	1667	96%	9	54%	-1657
7(b)	Defect size	1 + σ	3A	55%	1485	91%	29	36%	-1456
7(c), 2–6	Defect size	1 – σ	2A	48%	1995	93%	37	45%	-1958
7(d)	Sup./med. migration	2	2B	46%	12,394	76%	84	30%	-12,311
7(e)	Sup./med. migration	2 + σ	3B	50%	28,527	46%	3211	-4%	-25,316
7(f)	Sup./med. migration	2 – σ	2A	46%	1638	79%	188	34%	-1449
7(g)	Post./ante. orientation	3	2B	26%	9495	64%	571	38%	-8924
7(h)	Post./ante. orientation	3 + σ	3B	40%	16,288	60%	1252	20%	-15,036
8(i)	Post./ante. orientation	3 – σ	2C	69%	8957	83%	60	14%	-8896
8(j)	Inferior rim involvement	4	3B	42%	12,751	71%	340	29%	-12,411
8(k)	Inferior rim involvement	4 + σ	3B	86%	8791	71%	100	-15%	-8691
8(l)	Inferior rim involvement	4 – σ	3B	57%	1576	86%	14	29%	-1562
8(m)	Outer rim involvement	5	3A	50%	1459	94%	5	44%	-1455
8(n)	Outer rim involvement	5 + σ	2B	48%	30,251	69%	775	21%	-29,476
8(o)	Outer rim involvement	5 – σ	2C	52%	1760	89%	16	37%	-1745

fall into two categories: patient-adapted and patient-specific solutions.

Products like Zimmer Biomet's Trabecular Metal Acetabular Revision System (TMARS) allow surgeons to create patient-adapted solutions from a set of standard components, such as cups, buttresses, shims, and cages.[6] These systems offer better structural support than generic cups but are limited in terms of their ability to accurately match defect morphology by the finite number of available configurations. In severe cases, where statistical models fail to accurately capture pelvic defects, such an approach will likely have limited success. Moreover, the associated surgical technique, which involves the sequential assembly of an algorithmically defined set of components, is blind to the quality of the contact between the implant and the host bone surface. In fact, due to the nature of the assembly process, intra-operative component stability is likely the result of point contact, rather than area contact. Point contact is inherently less stable than area contact as it produces stress concentrations, and does not provide ideal conditions for long-term stability or bone ingrowth. Furthermore, augments are cemented to the central cup, making them susceptible to loosening through cyclical tensile and shear loading. Studies have observed augment loosening, and have associated contact between loose and stable augments with progressive metal debris shedding.[23] Others have also associated TMARS with significantly higher bone loss due to reaming than other custom implants.[24]

Existing patient-specific solutions, designed from scans of the patient's specific bone morphology, are typically reserved for severe cases in which the remaining bone stock is deemed insufficient for generic implants or TMARS. While the proposed system is intended as an alternative to TMARS, the enhanced bone preservation may enable its use even in cases where the patient would not have been a candidate for TMARS, due to an anticipated insufficiency of supporting bone stock post-reaming. Patient-specific solutions offered to TMARS candidates, such as Materialise's aMace, extend the outer surface of the cup to rest on the medial portion of the acetabulum, apparently through linear projection. Since details on the design process have not been published, a specific comparison with the proposed methodology is impossible at this time.

The proposed approach stands out for its ability to provide the benefits of other patient-specific or patient-adapted solutions, without the high design and procedural costs. As an alternative to TMARS, this approach would likely lead to better implant stability with less bone loss, while eliminating the need for intraoperative adjustments and cementing of the modular assembly.

Despite these advantages, the proposed method is limited by the quality of the input data, as well as the accuracy of the production method and operative technique. In particular, the reliability of the geometric bone reconstruction from CT data is limited by the accuracy and precision of the scanner, and can be affected by metal artifacts,[25] among other factors.[26] Additionally, the sclerotic or necrotic cancellous bone may be misidentified as healthy, resulting in an inaccurate reconstruction. The latter issue would potentially decrease the effective interface contact area, but would not hinder

insertability. Metal artifacts, however, may result in an uninsertable design, if not properly accounted for. This could potentially be addressed by incorporating computational artifact reduction techniques.[27–29] As a last resort, improper fit or contact could be addressed intra-operatively by using a (robot-assisted) vision system to inspect the cavity and perform additional minor bone resection if indicated.

A limitation of this study was that defect reconstructions were used as ground truth, without consideration for the possibility of inaccuracy introduced from the CT or surface reconstruction. Though the consequences may be mitigated intra-operatively, this limits the generalizability of the results presented herein.

This study also introduced an automatic sizing and placement strategy for the reference hemispherical cups which may not perfectly correspond with current practices. In particular, the algorithm favored larger cups for improved contact area, at the expense of bone loss. A surgeon may, instead, opt for a more conservative approach using a smaller diameter cup. This may, however, decrease the achievable interface contact.

In some samples such as Figure 7e, the large discontinuity on the acetabular fossa limits the achievable contact area and the structural integrity of the bone-implant system. Such cases may be better suited to more comprehensive treatments, such as CTACT or cup-cage reconstruction. Nonetheless, standard hemispherical components were used as a reference, for consistency.

This study also did not include a quantitative comparison between the proposed design strategy and existing patient-specific component systems, such as TMARS and CTAC. The complexity of these systems and the impact of uncontrolled factors, such as surgical expertise, would require a larger study, and would likely need to be performed in vivo.

The placement of fasteners, such as locking screws, was also omitted in the analysis. This aspect was ignored as the process is largely similar to standard hemispherical cups. However, the proposed approach provides more flexibility since screws may be positioned to target healthy bone stock. Standard line-of-sight algorithms[30] can be employed to ensure that holes are placed in reachable positions.

Finally, this study did not include a structural analysis of the stress conditions in the bone-implant system. Though not thought to be part of the standard design process for other patient-specific implants, stress conditions in the peri-prosthetic bone play an important role in long-term implant stability and bone health.

Despite these limitations, this study makes a strong case for the proposed patient-specific design strategy. In addition to the demonstrated performance improvements in terms of interface contact and bone preservation, the automated design strategy promises to be significantly less resource-intensive than existing patient-specific options.

AUTHOR CONTRIBUTIONS

ORCID

Eric Garner http://orcid.org/0009-0002-2323-5833

REFERENCES

1. OECD. *Health at a Glance 2021: OECD Indicators*. OECD Publishing; 2021.
2. Sloan Matthew, Prekumar Ajay, Sheth NeilP. Projected of primary total joint arthroplasty in the US, 2014 to 2030. *JBJS*. 2018;100.17:1455-1460.
3. Paprosky WG, O'Rourke M, Sporer SM. The treatment of acetabular bone defects with an associated pelvic discontinuity. *Clin Orthop Relat Res*. 2005;441:216-220.
4. Fryhofer GW, Ramesh S, Sheth NP. Acetabular reconstruction in revision total hip arthroplasty. *J Clin Orthop Trauma*. 2020;11:22-28.
5. Sheth NP, Nelson CL, Springer BD, Fehring TK, Paprosky WG. Acetabular bone loss in revision total hip arthroplasty: evaluation and management. *J Am Acad Orthop Surg*. 2013;21:128-139.
6. Trabecular metal acetabular revision system. Accessed April 23, 2024. www.zimmerbiomet.com,; https://www.zimmerbiomet.com/en/products-and-solutions/specialties/hip/trabecular-metal-acetabular-revision-system.html
7. Whitehouse MR, Masri BA, Duncan CP, Garbuz DS. Continued good results with modular trabecular metal augments for acetabular defects in hip arthroplasty at 7 to 11 years. *Clin Orthop Relat Res*. 2015;473:521-527.
8. Sporer SM, Paprosky WG. The use of a trabecular metal acetabular component and trabecular metal augment for severe acetabular defects. *J Arthroplasty*. 2006;21:83-86.
9. Lingaraj K, Teo YH, Bergman N. The management of severe bone defects in revision hip arthroplasty using modular porous metal components. *J Bone Jt Surg*. 2009;91.12:1555-1560.
10. Broekhuis D, Meurs W, Kaptein BL, et al. High accuracy of positioning custom triflange acetabular components in tumour and total hip arthroplasty revision surgery. *Bone Jt Open*. 2024;5:260-268. doi:10.1302/2633-1462.54.BJO-2023-0185.R1
11. Garner E, Wu J, Zadpoor AA. An insertability constraint for shape optimization. *Struct Multidisciplin Optimiz*. 2023;66:220.
12. Meynen A, Matthews H, Nauwelaers N, Claes P, Mulier M, Scheys L. Accurate reconstructions of pelvic defects and discontinuities using statistical shape models. *Comput Methods Biomech Biomed Engin*. 2020;23:1026-1033.
13. Meynen A, Vles G, Zadpoor AA, Mulier M, Scheys L. The morphological variation of acetabular defects in revision total hip arthroplasty – a statistical shape modeling approach. *J Orthop Res*. 2021;39:2419-2427.
14. American Joint Replacement Registry (AJRR): 2022 Annual Report. Rosemont, IL: American Academy of Orthopaedic Surgeons (AAOS), 2022. 51.
15. Lindahl H, Malchau H, Herberts P, Garellick G. Periprosthetic femoral fractures: classification and demographics of 1049 periprosthetic femoral fractures from the Swedish National Hip Arthroplasty Register. *J Arthroplasty*. 2005;20(7):857-865.
16. Ong KL, Kurtz SM, Lau E, Bozic KJ, Berry DJ, Parvizi J. Prosthetic joint infection risk after total hip in the Medicare population. *J Arthroplasty*. 2009;24(6):105-109.
17. Bozic KJ, Kurtz SM, Lau E, Ong K, Vail TP, Berry DJ. The epidemiology of revision total hip arthroplasty in the United States. *J Bone Jt Surg*. 2009;91:128-133.
18. Paprosky WG, Perona PG, Lawrence JM. Acetabular defect classification and surgical reconstruction in revision arthroplasty: a 6-year follow-up evaluation. *J Arthroplasty*. 1994;9.1:33-44.
19. Dalton JE, Cook SD, Thomas KA, Kay JF. The effect of operative fit and hydroxyapatite coating on the mechanical and biological response to porous implants. *J Bone Jt Surg*. 1995;77:97-110.
20. Haglin JM, Eltorai AEM, Gil JA, Marcaccio SE, Botero-Hincapie J, Daniels AH. Patient-Specific orthopaedic implants. *Orthop Surg*. 2016;8:417-424.
21. DeHaan AM, Adams JR, DeHart ML, Huff TW. Patient-specific versus conventional instrumentation for total knee arthroplasty: perioperative and cost differences. *J Arthroplasty*. 2014;29:2065-2069.
22. Watters TS, Mather RC, Browne JA, Berend KR, Lombardi AV Jr, Bolognesi MP. Analysis of procedure-related costs and proposed benefits of using patient-specific approach in total knee arthroplasty. *J Surg Orthop Adv*. 2011;20:112-116.
23. Abolghasemian M, Tangsataporn S, Sternheim A, Backstein D, Safir O, Gross AE. Combined trabecular metal acetabular shell and augment for acetabular revision with substantial bone loss: a mid-term review. *Bone Jt J*. 2013;95-B:166-172.
24. Callary S, Barends J, Solomon LB, Nelissen R, Broekhuis D, Kaptein B Virtual biomechanical assessment of custom triflange and trabecular metal components to treat large acetabular defects. Orthopaedic Proceedings. The International Hip Society (IHS). oston, MA, USA, 17–20 May 2023, vol. 105.
25. Pauwels R, Stamatakis H, Bosmans H, et al. Quantification of metal artifacts on cone beam computed tomography images. *Clin Oral Implants Res*. 2013;24:94-99.
26. Stull KE, Tise ML, Ali Z, Fowler DR. Accuracy and reliability of measurements obtained from computed tomography 3D volume rendered images. *Forensic Sci Int*. 2014;238:133-140.
27. Boas FE, Dominik, F. CT artifacts: causes and reduction techniques. *Imag Med*. 2012;4:229-240.
28. Gjesteby L, De Man B, Jin Y, et al. Metal artifact reduction in CT: where are we after four decades? *IEEE Access*. 2016;4:5826-5849.
29. Wellenberg RHH, Hakvoort ET, Slump CH, Boomsma MF, Maas M, Streekstra GJ. Metal artifact reduction techniques in musculoskeletal CT-imaging. *Eur J Radiol*. 2018;107:60-69.
30. Davim JP, ed. Machining: Fundamentals and Recent advances. 2008.